

Review of finite-difference schemes for the 1D heat / diffusion equation

Author: Oliver Ong

1 Introduction

The heat / diffusion equation is a second-order partial differential equation that governs the distribution of heat or diffusing material as a function of time and spatial location. Crank (1975) provides a particularly in-depth analysis of the mathematics behind the diffusion equation.

With the advance of computer technology, numerical methods have seen increasing popularity due to its computational speed and ability to easily solve complex problems. Fletcher (1988) discusses several numerical methods used in solving the diffusion equation (as well as other fluid dynamic problems). One popular subset of numerical methods are finite-difference approximations due to their easy derivation and implementation. Ames (1977) and Mitchell (1969) provide extensive reviews on finite-difference methods for different classes of partial differential equations.

In this paper, we review some of the many different finite-approximation schemes used to solve the diffusion / heat equation and provide comparisons on their accuracy and stability.

2 The Diffusion equation

The one-dimensional diffusion equation is a parabolic second-order partial differential equation of the form

$$\frac{\partial \phi}{\partial t} - \kappa \frac{\partial^2 \phi}{\partial x^2} = 0 \quad (1)$$

where $\phi = \phi(x, t)$ is the density of the diffusing material at spatial location x and time t , and the parameter κ is the diffusion coefficient. This equation is also known as the heat equation, which this paper may refer to in certain contexts as it allows the author to describe certain boundary conditions in terms of the thermodynamics of a conducting rod.

The majority of this report will focus on numerical schemes solving diffusion equation with Dirichlet boundary conditions specified at $x = 0$ and $x = L$, where L is the length of the domain

$$\phi(0, t) = 0, \quad \phi(L, t) = 0 \quad (2)$$

Neumann and periodic boundary conditions will be discussed in later sections.

3 Finite-difference formulations

In finite-difference methods, the partial differential equations are approximated discretely. That is to say, the numerical solution is only defined at a finite number of points along the domain in which the partial differential equation is to be solved.

The finite-difference method discretizes the spatial points along the domain $[0, L]$ with step-size $\Delta x = \frac{L}{N-1}$ where N is equal to the number of spatial nodes. Since the solution to the diffusion equation ϕ is also time-dependent, that is, the solution also evolves with time, we must also discretize along the time domain $[0, T]$, where T is the time to which the numerical schemes will run until. The time domain is discretized with step-size $\Delta t = \frac{T}{M-1}$, where M equal to the number of temporal nodes.

Figure 1 shows an illustration outlining the domain for the solution to the diffusion equation. The solid black squares refer to points in the domain that one must compute using finite-difference approximations as the other points are either already known or easily calculated.

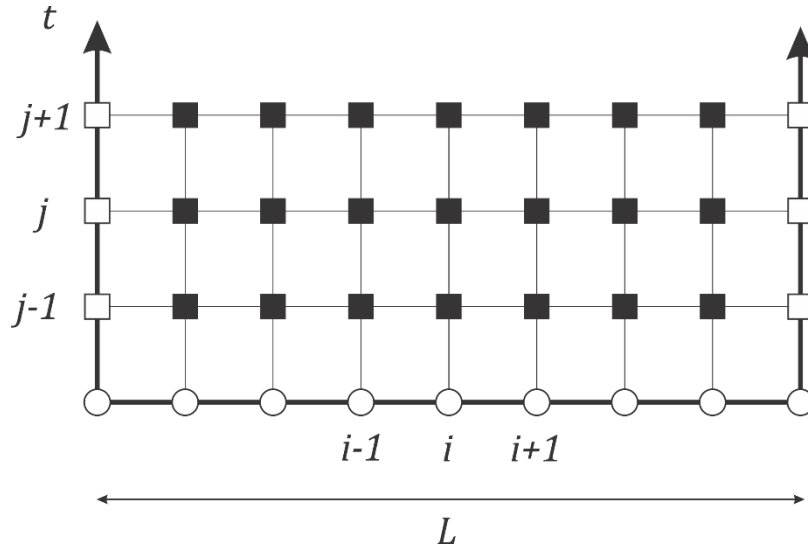


Figure 1 Discretization mesh for the solution to the 1-D diffusion equation. Open circles refer to known initial values, open squares refer to known boundary values, and solid squares refer to points where the values must be computed through finite-difference methods. The subscript i refers to discretization in the spatial domain, while the subscript j refers to discretization in the temporal domain.

Before we move onto the derivations of the different computational schemes, we must first find approximations to the continuous derivatives in Equation (1). In the table below, 3 first order derivative approximations are presented along with their respective truncation errors.

Table 1 Finite-difference approximations for the first order derivatives

Difference Approx.	Formula	Truncation Error
Forward Difference	$\frac{\partial \phi_i}{\partial x} = \frac{\phi_{i+1} - \phi_i}{\Delta x}$	$O(\Delta x)$
Backward Difference	$\frac{\partial \phi_i}{\partial x} = \frac{\phi_i - \phi_{i-1}}{\Delta x}$	$O(\Delta x)$
Central Difference	$\frac{\partial \phi_i}{\partial x} = \frac{\phi_{i+1} - \phi_{i-1}}{\Delta 2x}$	$O(\Delta x^2)$

Despite the central difference approximation being more accurate (lower truncation error), it cannot be easily implemented for finite-difference schemes as the equation does not include the ϕ_i term. Therefore, the forward and backward difference approximations are used as the time derivative in two of the finite-difference schemes reviewed later on.

Similarly, the central difference approximation for the second order spatial derivative has the same truncation error $O(\Delta x^2)$ and is defined as

$$\frac{\partial^2 \phi_i}{\partial x^2} = \frac{\phi_{i+1} - 2\phi_i + \phi_{i-1}}{\Delta x^2} \quad (3)$$

Now that we have approximations for the first and second order derivatives, we can develop the finite-difference schemes to compute the solution to the diffusion equation.

4 Forward-Time Central-Space

In this scheme as well as the other finite-difference methods, we will use the notation ϕ_i^j for the approximated solution where i refers to the spatial discrete index and j refers to the temporal discrete index.

A simple explicit scheme to solve the diffusion equation can be derived by simply substituting in the second order central and first order forward difference approximations for the continuous derivatives in space and time respectively

$$\frac{\phi_i^{j+1} - \phi_i^j}{\Delta t} = \kappa \frac{(\phi_{i-1}^j - 2\phi_i^j + \phi_{i+1}^j)}{\Delta x^2} \quad (4)$$

Solving for ϕ_i^{j+1} and setting

$$\alpha = \frac{\kappa \Delta t}{\Delta x^2} \quad (5)$$

produces the *Forward-Time Central-Space (FTCS)* scheme for approximating the solution to the diffusion / heat equation

$$\phi_i^{j+1} = \alpha(\phi_{i-1}^j + \phi_{i+1}^j) + (1 - 2\alpha)\phi_i^j \quad (6)$$

and results in a computational molecule illustrated as follows in Figure 2.

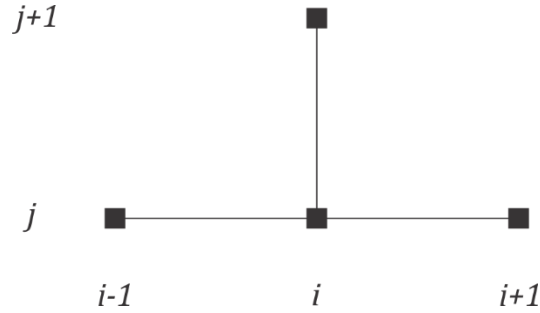


Figure 2 Computational molecule for the finite-difference Forward-Time Central-Space (FTCS) scheme

Stability Criterion

The dimensionless parameter α is known as the Courant number (Courant, et al., 1928), which in a physical sense may be seen as the number of spatial nodes that the heat or diffusing material can diffuse to in a time-step. Analysis of this parameter using Von Neumann stability analysis can provide insight to the stability of the FTCS scheme. Suppose we have a discretized solution of the form

$$\phi_k^l = e^{i\lambda\Delta x l} e^{\beta\Delta t k} \quad (7)$$

and we plug it into Equation (6). Doing so outputs the equation

$$e^{\beta\Delta t} = 1 - 4\alpha \sin^2\left(\frac{\lambda\Delta x}{2}\right) \quad (8)$$

Since $e^{\beta\Delta t} \leq 1$, we can show that,

$$\alpha = \frac{\kappa\Delta t}{\Delta x^2} \leq \frac{1}{2} \quad (9)$$

Thus, the explicit FTCS scheme remains stable as long as the Courant number is less than or equal to 1/2. If the parameter is set above this value, the algorithm becomes unstable with growing oscillations. This effectively limits the size of the time-steps to relatively small values. We'll see in the following sections that this is not the case for implicit schemes.

5 Backward-Time Central-Space

The derivation of the implicit *Backward-Time Central Space (BTCS)* scheme is similar to the FTCS, except that the backward difference is used on the time derivative instead of the forward difference

$$\frac{\phi_i^j - \phi_i^{j-1}}{\Delta t} = \kappa \frac{(\phi_{i-1}^j - 2\phi_i^j + \phi_{i+1}^j)}{\Delta x^2} \quad (10)$$

Another difference is that for the FTCS scheme, an explicit equation exists to solve for each point whereas in the BTCS scheme, we must simultaneously solve a set of equations over the whole spatial domain at each time-step. If we rearrange Equation (10) to separate the points associated with each time-step, we produce the equation

$$\phi_i^{j-1} = -\alpha\phi_{i-1}^j + (1 + 2\alpha)\phi_i^j - \alpha\phi_{i+1}^j \quad (11)$$

which can be represented as a systems of equation as

$$\begin{bmatrix} 1 + 2\alpha & -\alpha & 0 & 0 & 0 & 0 \\ -\alpha & 1 + 2\alpha & -\alpha & 0 & 0 & 0 \\ 0 & -\alpha & 1 + 2\alpha & -\alpha & 0 & 0 \\ 0 & 0 & \ddots & \ddots & \ddots & 0 \\ 0 & 0 & 0 & -\alpha & 1 + 2\alpha & -\alpha \\ 0 & 0 & 0 & 0 & -\alpha & 1 + 2\alpha \end{bmatrix} \begin{bmatrix} \phi_1^j \\ \phi_2^j \\ \phi_3^j \\ \vdots \\ \phi_{N-1}^j \\ \phi_N^j \end{bmatrix} = \begin{bmatrix} \phi_1^{j-1} \\ \phi_2^{j-1} \\ \phi_3^{j-1} \\ \vdots \\ \phi_{N-1}^{j-1} \\ \phi_N^{j-1} \end{bmatrix} \quad (12)$$

The associated computational molecule for this scheme is illustrated below in Figure 3.

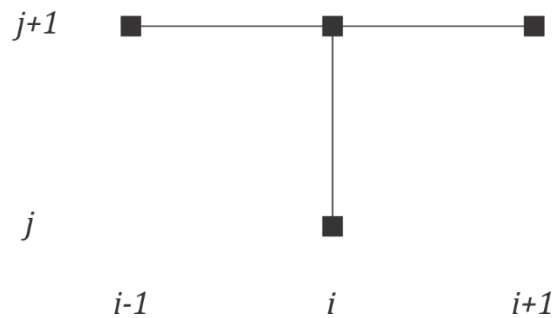


Figure 3 Computational molecule for the finite-difference Backward-Time Central-Space (BTCS) scheme

Stability Criterion

Von Neumann stability analysis of this scheme is similar to that of the FTCS, except we plug in Equation (7) into Equation (11) instead. Doing so yields the following

$$e^{\beta\Delta t} = \frac{1}{1 + 4\alpha \sin^2\left(\frac{\lambda\Delta x}{2}\right)} \quad (13)$$

which implies that the BTCS scheme is unconditionally stable for $\alpha > 0$. This is true for all implicit finite-difference schemes, including the Crank-Nicolson scheme to be discussed in the next section.

6 Crank-Nicolson

The implicit *Crank-Nicolson* (C-N) scheme is similar to the BTCS with a slight difference in approximating the spatial derivative. The Crank-Nicolson method (Crank & Nicolson, 1947) computes the spatial derivative with an average of the central difference approximation at the current and previous time-step, resulting in a scheme that has a temporal truncation error of $O(\Delta t^2)$

$$\frac{\phi_i^j - \phi_i^{j-1}}{\Delta t} = \frac{\kappa}{2} \left[\frac{(\phi_{i-1}^j - 2\phi_i^j + \phi_{i+1}^j)}{\Delta x^2} + \frac{(\phi_{i-1}^{j-1} - 2\phi_i^{j-1} + \phi_{i+1}^{j-1})}{\Delta x^2} \right] \quad (14)$$

Rearranging Equation (14) to isolate the points associated with each time-step results in the following

$$-\frac{\alpha}{2}\phi_{i-1}^j + (1 + \alpha)\phi_i^j - \frac{\alpha}{2}\phi_{i+1}^j = (1 - \alpha)\phi_i^{j-1} + \frac{\alpha}{2}(\phi_{i-1}^{j-1} + \phi_{i+1}^{j-1}) \quad (15)$$

The matrix representation of this equation is similar to that of the BTCS scheme

$$\begin{bmatrix} 1 + \alpha & -\alpha/2 & 0 & 0 & 0 & 0 \\ -\alpha/2 & 1 + \alpha & -\alpha/2 & 0 & 0 & 0 \\ 0 & -\alpha/2 & 1 + \alpha & -\alpha/2 & 0 & 0 \\ 0 & 0 & \ddots & \ddots & \ddots & 0 \\ 0 & 0 & 0 & -\alpha/2 & 1 + \alpha & -\alpha/2 \\ 0 & 0 & 0 & 0 & -\alpha/2 & 1 + \alpha \end{bmatrix} \begin{bmatrix} \phi_1^j \\ \phi_2^j \\ \phi_3^j \\ \vdots \\ \phi_{N-1}^j \\ \phi_N^j \end{bmatrix} = \begin{bmatrix} a_1 \\ a_2 \\ a_3 \\ \vdots \\ a_{N-1} \\ a_N \end{bmatrix} \quad (16)$$

where the coefficients a_i can be computed as

$$a_i = (1 - \alpha)\phi_i^{j-1} + \frac{\alpha}{2}(\phi_{i-1}^{j-1} + \phi_{i+1}^{j-1}) \quad (17)$$

The computational molecule associated with this scheme is illustrated below in Figure 4.

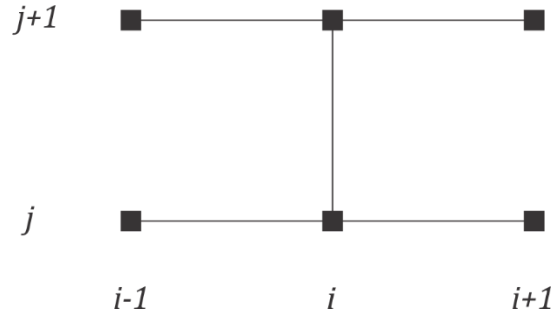


Figure 4 Computational molecule for the finite-difference Crank-Nicolson (C-N) scheme

7 Stability comparison

In this section, the three finite-difference schemes are implemented with Dirichlet conditions $\phi(0, t) = \phi(L, t) = 0$ with an initial condition $\phi(x, 0) = \sin\left(\frac{\pi x}{L}\right)$ to verify the stability criterion derived for the various schemes.

Figure 5 shows the *Forward-Time Central-Space (FTCS)* scheme implemented with 100 spatial nodes and Courant number $\alpha = 0.5$ at different times along the simulation. The solution ran until

the end time of 2.5 seconds without producing any oscillations. The accuracy of these approximations will be considered in the following section.

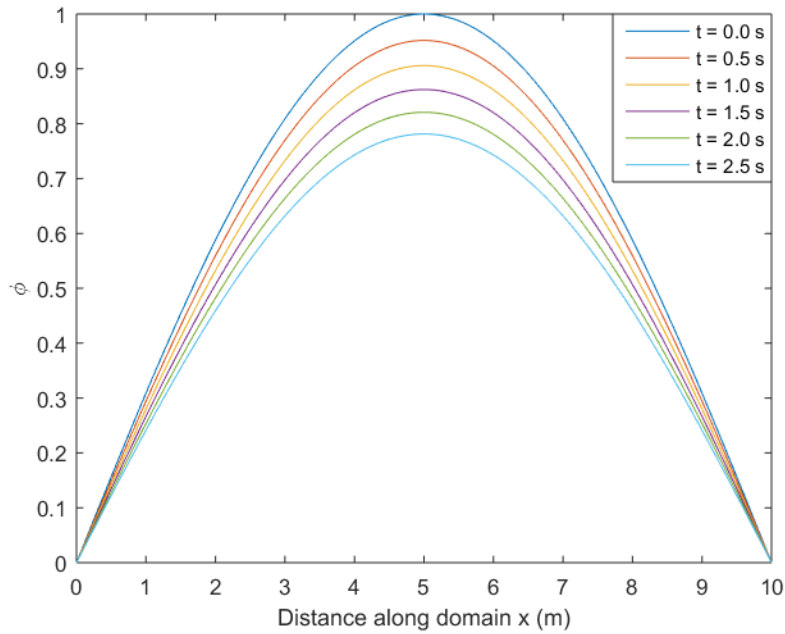


Figure 5 Forward-Time Central-Space (FTCS) approximation to the diffusion / heat equation evaluated at different times. Implemented with Dirichlet boundary conditions. $\alpha = 0.5$

While keeping the initial and boundary conditions constant from the previous simulation, we vary the Courant number α to be greater than 0.5, we start to see oscillations in the approximation grow as the time evolves.

Figure 6 shows the FTCS scheme implemented with $\alpha = 1$ evaluated at different times and shows that oscillations are produced in the numerical solution. These oscillations are more apparent at this scale from approximately $t = 0.30$ s.

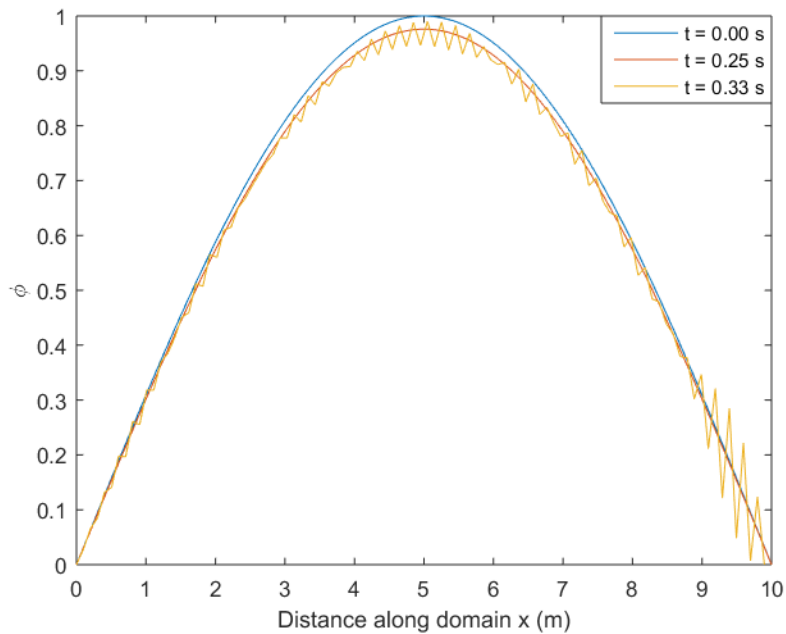


Figure 6 Forward-Time Central-Space (FTCS) approximation to the diffusion / heat equation evaluated at different times. Implemented with Dirichlet boundary conditions. $\alpha = 1$

As the oscillations tend to grow exponentially with time, only 3 time-points were evaluated for this figure in order to keep the scale of the plot consistent with Figure 5.

Next, we will implement the implicit methods with the same initial and boundary conditions for $\alpha = 1$. Figure 7 shows the approximations of these two methods evaluated at different time-points.

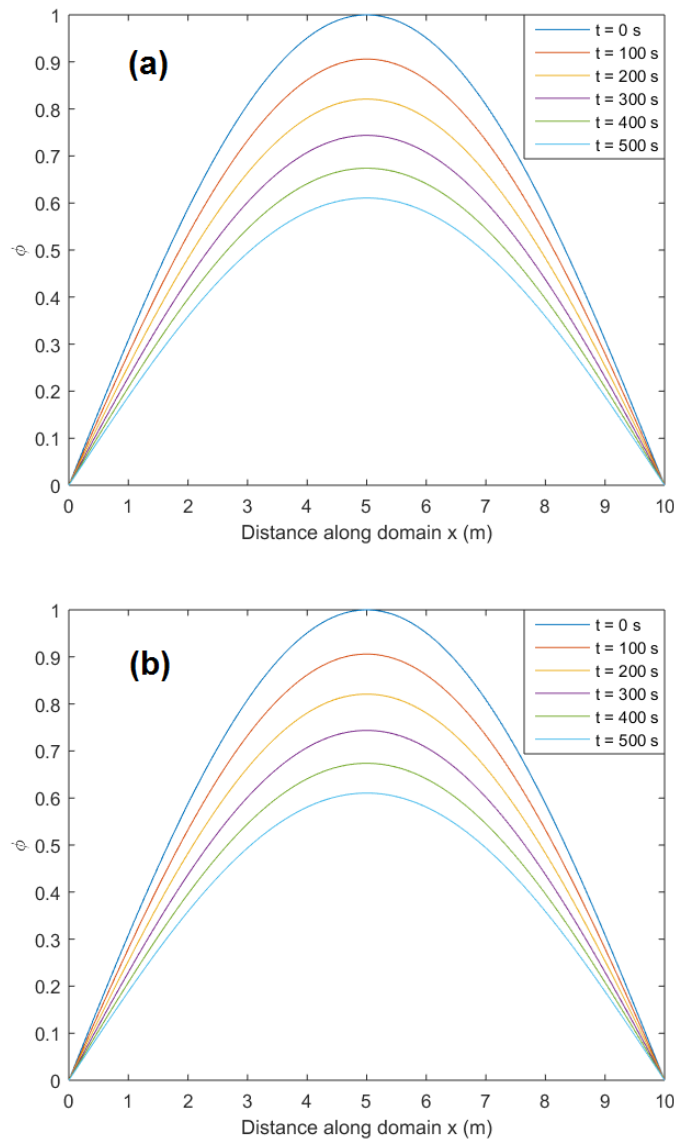


Figure 7 (a) Backwards-Time Central-Space (BTCS) and (b) Crank-Nicolson (C-N) approximations to the diffusion / heat equation evaluated at different times. Implemented with Dirichlet boundary conditions, $\alpha = 1$

Both BTCS and Crank-Nicolson approximations provide consistent results without any oscillations. This supports our claim on the unconditional stability of the two schemes.

8 Accuracy

In order to determine the relative accuracy of each method, the truncation errors for each scheme are compared. Using the initial condition and the Dirichlet BC stated in Section 6, we derive the exact time-dependent solution

$$\phi(x, t) = \sin\left(\frac{\pi x}{L}\right) e^{-\kappa\left(\frac{\pi}{L}\right)^2 t} \quad (18)$$

To provide estimates of the truncation error, the L_2 norm between the approximated and exact solution is calculated for each scheme at the end time of the simulation

$$\epsilon = \|\phi_i - \phi_{exact}(x_i, t_i)\|_2 \quad (19)$$

Figure 8 plots the error in L_2 norm for the three finite-difference schemes as a function of the spatial step-size.

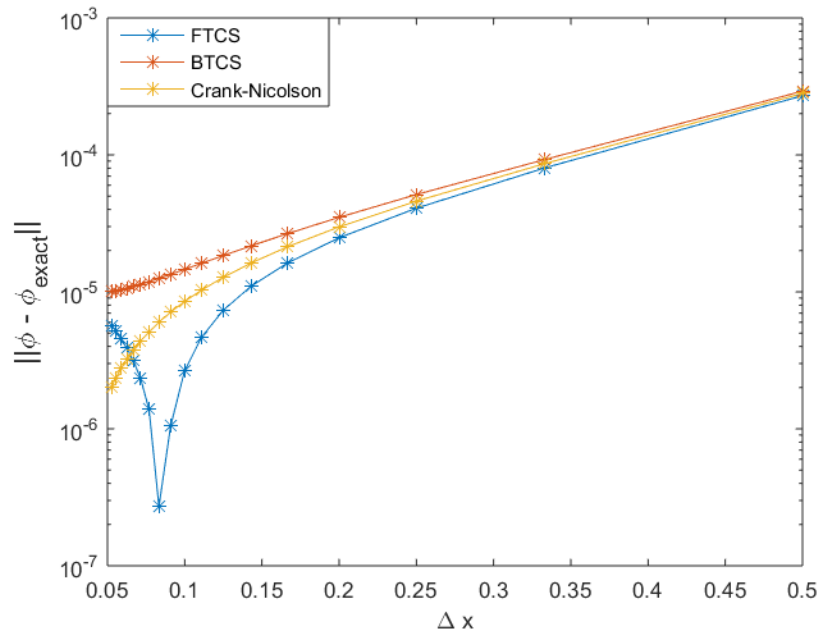


Figure 8 Error in L_2 norm plotted as a function of spatial step-size. $\Delta t = 0.001$ s, $\kappa = 1$

The accuracy of each method appears to be largely dependent on the spatial step-size used in the scheme. The plot shows that as the spatial step-size decreases, both BTCS and Crank-Nicolson

approximations increase in accuracy. The trend for the FTCS scheme shows that for small spatial step-size, the truncation error first decreases before increasing past that of the Crank-Nicolson scheme.

These results are consistent with the results of Dehghan (2004) that show the FTCS scheme providing slightly more accurate approximations with decreased spatial step-size and constant Courant number.

9 Boundary Conditions

So far, we've only discussed approximations for the diffusion / heat equation with Dirichlet boundary conditions. In this section, we will consider other types of boundary conditions and discuss details of implementing these for the different schemes.

Neumann boundary conditions

For Dirichlet boundary conditions (also known as fixed boundary conditions), the endpoints of the spatial domain of the solution are explicitly specified as values. Neumann boundary conditions, on the other hand, specify values that the derivative of the solution would impose. This would be equivalent to specifying the heat flux at the boundaries in the context of the heat equation.

Mixed boundary conditions

Mixed boundary conditions specify different types of boundary conditions (Dirichlet and Neumann) at the end nodes of the solution. For example, we could have a Dirichlet BC at the left boundary and values corresponding to a Neumann BC on the right boundary. In the context of the heat equation, this would be similar to holding one boundary at a fixed temperature (attached to a heat reservoir) and specifying the heat flux at the other.

Robin boundary conditions

These boundary conditions are considered to be a weighted mixture of Dirichlet and Neumann boundary conditions and tend to take the form

$$\phi = a_0 + b_0 \frac{\partial \phi_i}{\partial x}$$

where i can refer to the 1 (left boundary) or L (right boundary) with coefficients a_0 and b_0 .

In the following sections, we will provide several solutions to the diffusion / heat equation using various boundary conditions.

10 Neumann boundary condition example

In this example, the solution to the heat equation is solved with Neumann boundary conditions on both ends of the spatial domain

$$\phi(0, t) = 3, \quad \phi(L, t) = 2 \quad (20)$$

In the context of the heat equation, this would correspond to the isolated boundaries of a rod. Using the same initial condition

$$\phi(x, 0) = \cos\left(\frac{\pi x}{2L}\right) + 2 \quad (21)$$

the solution to the heat equation is approximated with the Crank-Nicolson scheme in Figure 9.

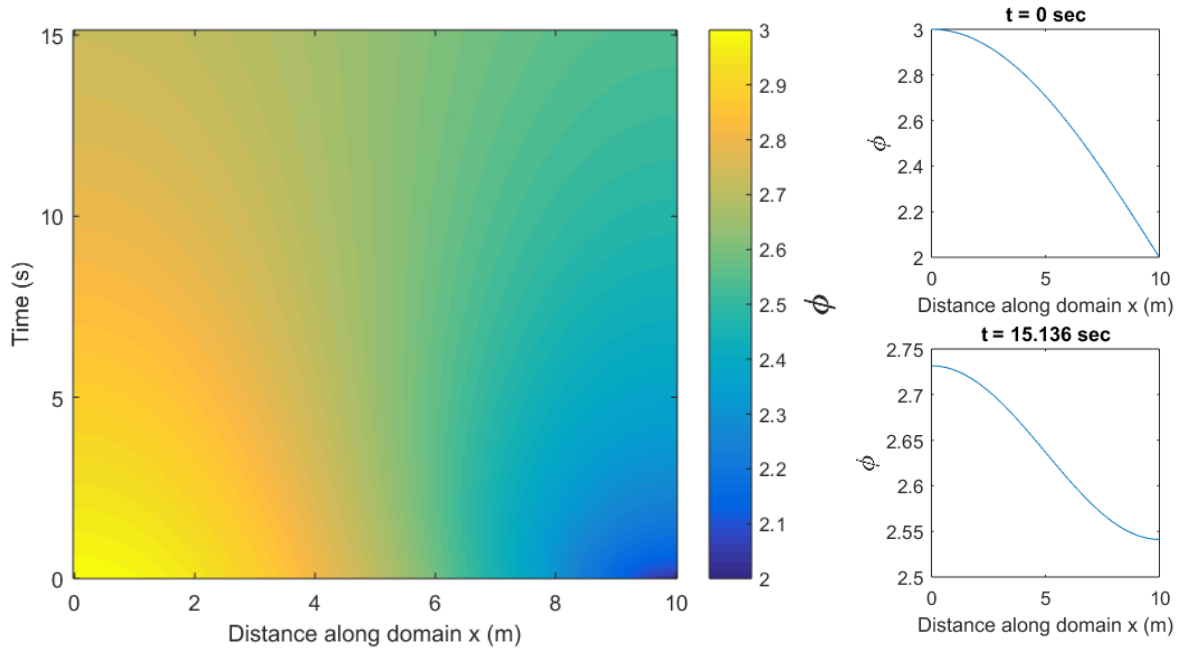


Figure 9 Crank-Nicolson (C-N) approximated solution to the diffusion / heat equation as a function of spatial distance and time. Neumann boundary conditions applied. Solution at initial and end times shown.

11 Robin boundary condition example

With the same initial condition as in the previous section, we now provide an example of a solution with Robin boundary conditions

$$\frac{\partial \phi(0, t)}{\partial x} = \beta \phi(0, t), \quad \phi(L, t) = 2 \quad (22)$$

For the heat equation, these conditions correspond to a heat flux value proportional to the temperature at the left boundary and the constant β . The right boundary is held fixed (Dirichlet), corresponding to a rod in contact with a heat reservoir of temperature 2 K. The solution to this problem is again approximation by the Crank-Nicolson scheme in Figure 10.

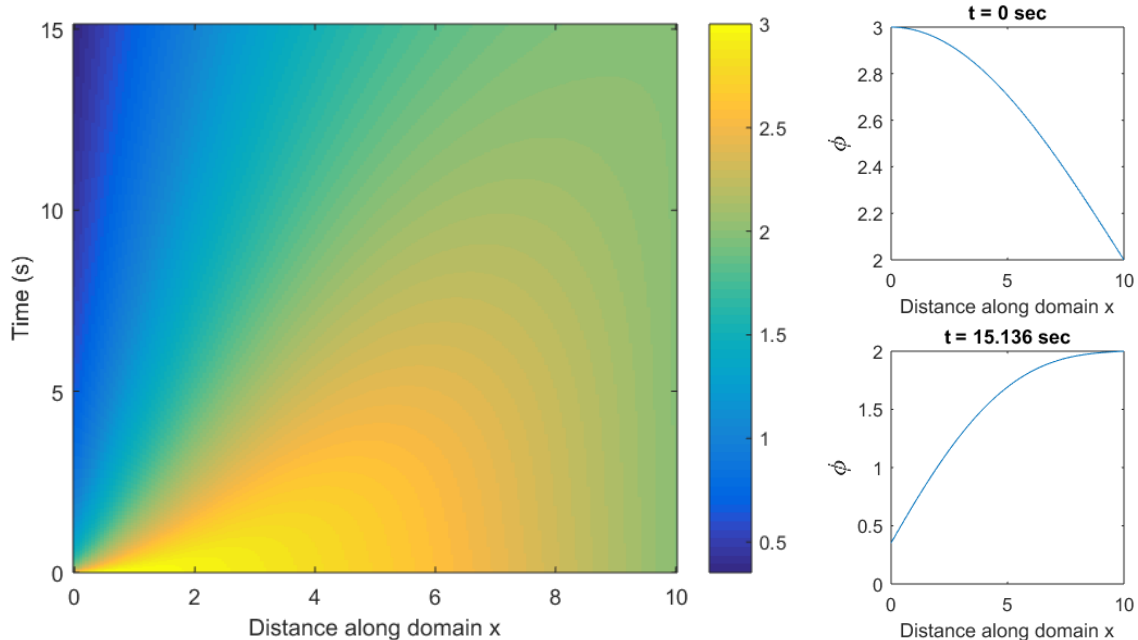


Figure 10 Crank-Nicolson (C-N) approximated solution to the diffusion / heat equation as a function of spatial distance and time. Robin boundary conditions applied. Solution at initial and end times shown.

12 Lowest Eigenvalue problem

The lowest eigenvalue for the solution to the heat equation is proportional to the decay rate of the solution. For this problem, we will consider an initial value problem with initial condition

$$\phi(x, 0) = \cos\left(\frac{\pi x}{L}\right) \quad (23)$$

with Dirichlet boundary conditions

$$\phi(0, t) = 1, \quad \phi(L, t) = -1 \quad (24)$$

The Crank-Nicolson scheme is used to approximate the solution to an arbitrary point in time. Simultaneously, the steady state solution of the form

$$\phi(x) = \frac{\phi(0) - \phi(L)}{L}x + \phi(0) \quad (25)$$

is subtracted from the time-dependent solution. Figure 11 shows the approximated solution at $t = 0$ as well as the difference between the approximated and steady state solution.

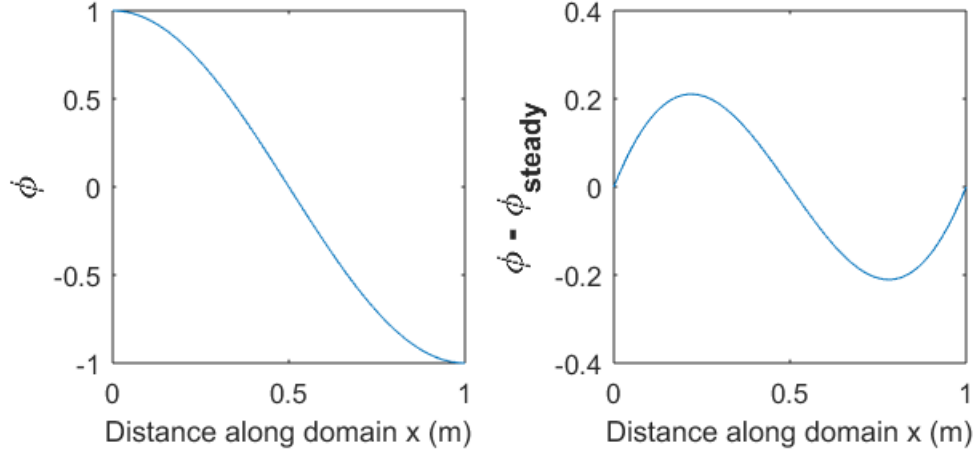


Figure 11 Plots of the approximated time-dependent solution using C-N scheme (left) and the difference between the approximated solution and steady-state solution (right). Computed at $t = 0$

The solution with the steady state subtracted decays exponentially with time for which the decay rate is proportional to the lowest eigenvalue

$$\lambda_1 = \kappa \left(\frac{\pi}{L} \right)^2 \quad (26)$$

13 Conclusion

In this paper, three finite-difference schemes are reviewed and implemented for the one-dimensional diffusion / heat equation for different initial and boundary conditions. Stability analysis for the different schemes showed that the explicit Forward-Time Central-Space (FTCS) scheme is unstable for Courant numbers greater than 0.5 while implicit schemes such as the Backward-Time Central-Space (BTCS) and Crank-Nicolson (C-N) are unconditionally stable. Implementation of these schemes with varied Courant numbers verified these claims as the FTCS method produced growing oscillations in the solution with time while the implicit schemes (BTCS and C-N) did not. To compare the accuracy of each method, the error of L2 norms of the different methods were computed. The results showed that the relative accuracy of the schemes were largely dependent on the spatial step-size used. As the step-size decreased, the Crank-Nicolson scheme

produced solutions with lower truncation errors. An eigenvalue problem for the diffusion / heat equation was also presented in this paper attempting to relate the decay rate of the approximated solution to the lowest eigenvalue. Although the theory shows that the two variables may be proportional to each other, numerical approaches to prove this claim were unfortunately unsuccessful.

References

- Ames, W. F., 1977. *Numerical Methods for Partial Differential Equations*. 1 ed. New York : Academic Press.
- Courant, R., Friedrichs, K. & Lewy, H., 1928. Über die partiellen Differenzgleichungen der mathematischen Physik. *Mathematische Annalen*, 100(1), pp. 32-74.
- Crank, J., 1975. *The Mathematics of Diffusion*. 2nd ed. London: Oxford University Press.
- Crank, J. & Nicolson, P., 1947. A practical method for numerical evaluation of the solutions of partial differential equations of the heat-conduction type. *Mathematical Proceedings of the Cambridge Philosophical Society*, 43(01), pp. 50-67.
- Dehghan, M., 2004. Numerical schemes for one-dimensional parabolic equations with nonstandard initial condition. *Applied Mathematics and Computation*, 147(1), pp. 321-331.
- Fletcher, C., 1988. *Computational Techniques for Fluid Dynamics I*. 1 ed. Berlin; New York: Springer-Verlag.
- Mitchell, A. R., 1969. *Computational methods in partial differential equations*. 1 ed. London: Wiley.

Figure 1 Discretization mesh for the solution to the 1-D diffusion equation. Open circles refer to known initial values, open squares refer to known boundary values, and solid squares refer to points where the values must be computed through finite-difference methods. The subscript i refers to discretization in the spatial domain, while the subscript j refers to discretization in the temporal domain.....	3
Figure 2 Computational molecule for the finite-difference Forward-Time Central-Space (FTCS) scheme.....	5
Figure 3 Computational molecule for the finite-difference Backward-Time Central-Space (BTCS) scheme.....	6
Figure 4 Computational molecule for the finite-difference Crank-Nicolson (C-N) scheme	8
Figure 5 Forward-Time Central-Space (FTCS) approximation to the diffusion / heat equation evaluated at different times. Implemented with Dirichlet boundary conditions. $\alpha = 0.5$	9
Figure 6 Forward-Time Central-Space (FTCS) approximation to the diffusion / heat equation evaluated at different times. Implemented with Dirichlet boundary conditions. $\alpha = 1$	10
Figure 7 (a) Backwards-Time Central-Space (BTCS) and (b) Crank-Nicolson (C-N) approximations to the diffusion / heat equation evaluated at different times. Implemented with Dirichlet boundary conditions, $\alpha = 1$	11
Figure 8 Error in L2 norm plotted as a function of spatial step-size. $\Delta t = 0.001$ s, $\kappa = 1$	12
Figure 9 Crank-Nicolson (C-N) approximated solution to the diffusion / heat equation as a function of spatial distance and time. Neumann boundary conditions applied. Solution at initial and end times shown.	15
Figure 10 Crank-Nicolson (C-N) approximated solution to the diffusion / heat equation as a function of spatial distance and time. Robin boundary conditions applied. Solution at initial and end times shown.....	16
Figure 11 Plots of the approximated time-dependent solution using C-N scheme (left) and the difference between the approximated solution and steady-state solution (right). Computed at $t = 0$	17